

PAPER • OPEN ACCESS

The effect of shell material and load coefficient on the expansion of shell driven by detonation

To cite this article: X Y Wang *et al* 2020 *J. Phys.: Conf. Ser.* **1507** 032045

View the [article online](#) for updates and enhancements.



The Electrochemical Society
Advancing solid state & electrochemical science & technology

The ECS is seeking candidates to serve as the
Founding Editor-in-Chief (EIC) of ECS Sensors Plus,
a journal in the process of being launched in 2021

The goal of ECS Sensors Plus, as a one-stop shop journal for sensors, is to advance the fundamental science and understanding of sensors and detection technologies for efficient monitoring and control of industrial processes and the environment, and improving quality of life and human health.

Nomination submission begins: May 18, 2021



Nominate now!

The effect of shell material and load coefficient on the expansion of shell driven by detonation

X Y Wang¹, Sh Sh Wang² and X Lu¹

¹Department of Equipment Engineering, Shenyang Ligong University, Liaoning Shenyang 110159, China

²State Key Laboratory of Explosion Science and Technology, Beijing Institute of Technology, Beijing, 100081, China

Email:13889858980@163.com

Abstract. Detonation driven metal expansion and fragmentation is a complex transient nonlinear dynamic problem. The research on the influence of the materials and load coefficients on expansion driven by detonation can provide a basis for fragment velocity prediction and warhead design. The numerical simulation of detonation driving was studied, including the TNT charge with five kinds of materials and six kinds of load coefficient β values shells. The characteristics in detail which the experiment was difficult to reflect were obtained, and the influence of material properties and β value of metal shells on the fragment velocities were revealed. With the increase of the density of the material, the dissipative energy of the shock wave in the casing decreases, and the contribution of the shock wave loading to the velocity of the fragment increases. Meanwhile, the increase of the shell wall thickness and the corresponding decrease of β value lead to the increase of the internal dissipation energy of the shock wave in the casings, the decrease of the energy for the shell expansion acceleration and the decrease of the contribution to the fragment velocity.

1. Introduction

The expansion and fracture of metal shell driven by detonation include explosive detonation, shock wave loading, detonation product expansion, metal accelerating movement until fracture, forming fragments with damage ability and other physical and chemical processes. The initial velocity of fragments reflects the effective energy of fragment load. Gurney [1] first proposed a classical model of fragment initial velocity. Based on the instantaneous detonation and energy conservation, it was assumed that the chemical energy of explosive will be converted into metal kinetic energy and detonation product kinetic energy after detonation, and a very simple and practical Gurney formula for calculating the initial velocity of cylindrical charge fragment was established. Lee [2] et al. proposed a method to calibrate Gurney velocity with standard cylinder test. Kury et al. [3] first proposed and applied the standard cylinder test, which was specially used to evaluate the working capacity of explosives and determine the JWL state equation and gurney energy of explosive detonation products.



According to the Gurney formula, the initial velocity of fragments only depends on the load coefficient β and the gurney velocity related to the explosive performance. When the explosive is fixed, the shell material and load coefficient β are the main factors affecting the initial velocity of fragments.

A large number of experimental phenomena have shown that [4-6] the metal shell had a very high acceleration in the initial stage of expansion, i.e. the expansion speed of the shell increases rapidly in a very short time. This fact and the remarkable oscillation characteristics of the expansion velocity showed that the shock wave formed by the detonation wave passing through the inner surface of the shell had an important influence on the detonation expansion and acceleration of the metal shell. In the detonation driving process, the combined action of shock wave and detonation product expansion drive the metal shell to accelerate, and part of the total energy was converted into metal kinetic energy. The theoretical research represented by the gurney model was based on the instantaneous detonation hypothesis and the law of conservation of energy, which essentially ignored the shock wave loading effect and the details of the expansion process of the detonation product and the metal shell. Moreover, the gurney energy of the explosive was obtained by the standard cylinder test under the specific shell material and structure size. However, the structure and shell material of warhead are different from the standard cylinder test in most cases, and the test data obtained from the experimental study were limited, so it was difficult to understand the essence of detonation driven metal expansion. Numerical simulation is an effective method to study the detonation driven metal problem. Combined with theory and experiment, in the range of acceptable error, the process of detonation driven metal expansion was studied by numerical simulation, which revealed the detailed expansion process that was difficult to reflect by limited experimental data, so as to realize a more comprehensive and detailed analysis of detonation driven metal problems. In addition, the simulation calculation can supplement a lot of repeated experimental work, provide data support for the regular analysis of detonation driven metal energy conversion problem, reduce the experimental consumption, and improve the research efficiency [7-10].

In this paper, the numerical model of the oxygen-free copper shell driven by detonation of TNT explosive was established by using AUTODYN, and compared with the experimental results in the literature. Thus, the rationality and applicability of numerical modeling and simulation methods were verified. The numerical simulation of the shells of five materials and six kinds of wall thickness shells driven by TNT cylindrical explosive were carried out. The effects of material properties and load coefficient β on fragment velocity were analyzed, and the details and essential characteristics of metal expansion acceleration driven by detonation were revealed.

2. Numerical simulation of metal shell driven by detonation

2.1. Numerical modeling

The metal cylinder driven by explosive detonation is of axisymmetric structure. In order to facilitate the calculation, the two-dimensional axisymmetric model is adopted. The inner diameter of the metal shell is Φ 50mm, the length is 240mm, and the outer diameter is calculated with the change of β value; the diameter of TNT grain is 50mm, and the length is 200mm; the plexiglass plug is placed at both ends, and its length is 20mm. The simulation model is shown in figure 1. The x-axis is the symmetry axis, and the length and width of the air domain are 340mm and 80mm respectively. The point

initiation method is adopted, and the initiation point is set at the center of the left end face of the explosive, i.e. the position of the explosion point in the figure. The air domain is constructed by Euler element, and the explosive and glass plug are filled. The metal shell adopts the Lagrange element with the grid density of 0.5mm, and the Euler / Lagrange fluid structure coupling connection mode should be selected between them. The outer boundary of the air region is set as the flow out boundary.

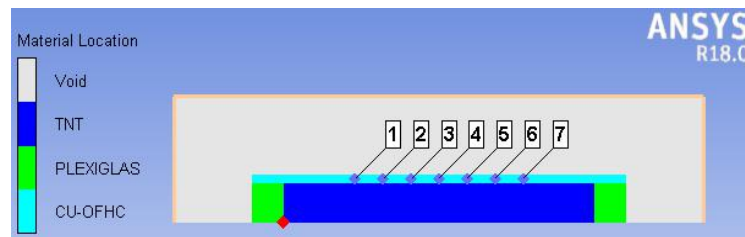


Figure 1. Simulation model.

2.2. Material model

TNT-2 is selected from the material bank, and the pressure in the detonation product is described by JWL equation of state,

$$p = A \left(1 - \frac{\omega}{R_1 V} \right) e^{-R_1 V} + B \left(1 - \frac{\omega}{R_2 V} \right) e^{-R_2 V} + \frac{\omega E}{V} \quad (1)$$

Where E is the internal energy per unit mass, V is the relative specific volume of the detonation product, and a, B, R1, R2 and ω are constants. The metal shell used in the numerical simulation process includes five kinds of metal materials: oxygen free copper, 45# steel, 50SiMnVB steel, TC4 titanium alloy and 6061 aluminum alloy. The material model is shown in table 1, which is mainly from AUTODYN material library, and the parameters are adjusted appropriately according to the experimental parameters.

Table 1. Material model and parameters of metal shells.

Shell material	$\rho / \text{g} \cdot \text{cm}^{-3}$	state equation	Johnson-Cook				
			A /MPa	B /MPa	n	C	m
copper	8.90	Linear	90	292	0.31	0.025	1.09
45# steel	7.85	Linear	792	510	0.26	0.014	1.03
50SiMnVB steel	7.85	Linear	615	588	0.408	0.034	1.03
TC4 Ti	4.5	Shock	800	0.0	0.0	0.011	1.0
6061 Al	2.7	Shock	345	462	0.25	0.01	1.0

2.3. Gauge point setting

In AUTODYN, the data is collected and analyzed by setting gauge points. In the simulation model, the Gauge points 1-7 are set at the center axis of the shell with an axial interval of 18mm from left to right, as shown in figure 1. In addition, Gauge points 8 and 9 are set on the inner and outer surface of the middle of the shell. Figure 2 shows the velocity curves at different Gauge points. It can be seen from figure 2 that the fluctuation difference in the front section of the velocity curve of the Gauge points 4,

8 and 9 located in the middle radial direction is obvious, but the difference is not significant after the velocity is stable. The front section of the velocity curve of Gauge point 1-7 located in the axial direction has basically the same change, but there is a difference in the velocity stable section. Because of the influence of the end effect, the velocity value near the initiation end is low, and it is basically the same after Gauge point 4, so the data of Gauge point 4 at the central axis of the shell expansion velocity acquisition is enough. Figure 3 is the pressure curve at different Gauge points. In the axial direction, the pressure slightly attenuates, and the attenuation amplitude is small, which can be ignored. However, the change of pressure on the inner and outer surface is obvious, which is caused by the attenuation of shock wave in the shell. The pressure at the center point can be selected for relative comparison. Therefore, it is more appropriate to set Gauge point on the central axis.

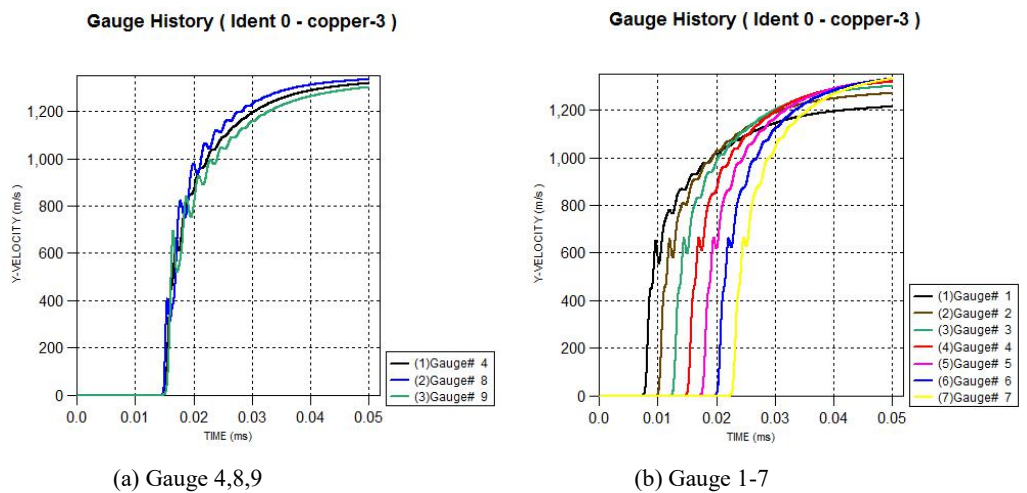


Figure 2. Velocity curves at different Gauge points.

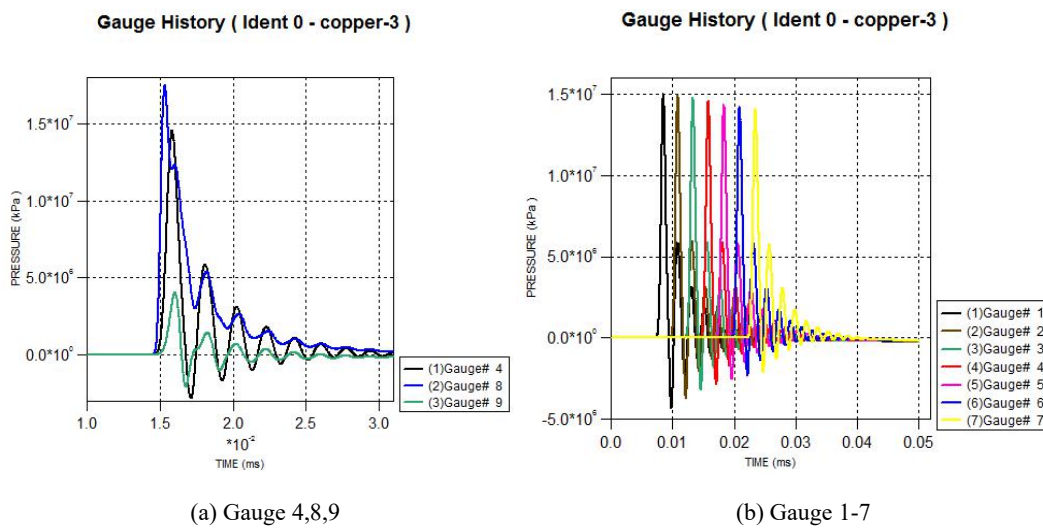


Figure 3. Pressure curves at different Gauge points.

3. Analysis of numerical simulation results

3.1. Effect of metal materials on the expansion process of metal shell driven by detonation

Five kinds of metal shells with $\beta = 0.34$ are selected for simulation. Figure 4 shows the external surface velocity and displacement curve of the oxygen-free copper shell obtained by numerical simulation. Compared with the experimental data curve in reference [11], it can be seen that the simulation results are in good agreement with the experimental results, which verifies the rationality and practicability of the numerical model and method.

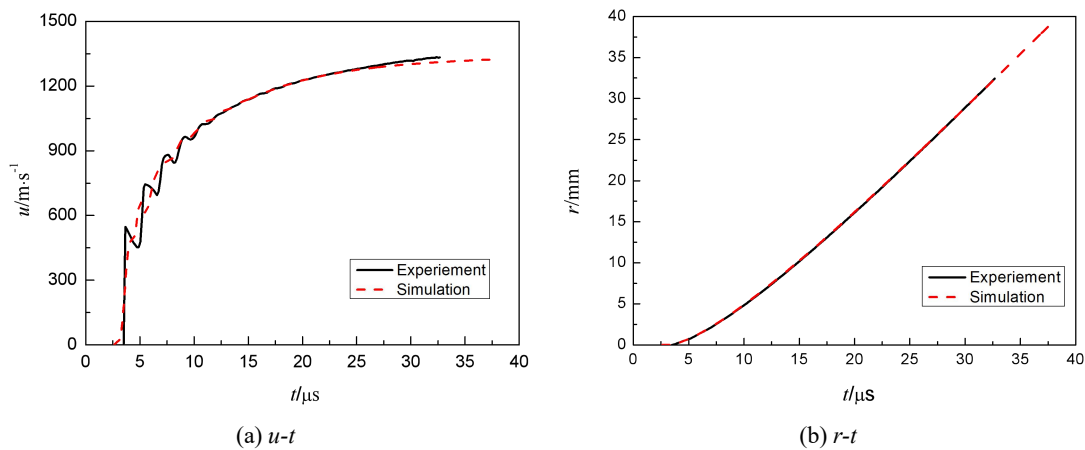


Figure 4. Contrast curves between experimental and simulation of velocity and displacement on outer surface of copper shell.

The expansion speed curve and pressure curve of five materials shell are calculated with $\beta = 0.34$, as shown in figure 5. Gauge point 4 is selected at the middle axis of the shell for analysis. Table 2 shows the maximum expansion speed of the shell and the maximum pressure in the shell. It can be seen from the comparison of velocity curves that, due to the same charge, the same explosion load, the time when the velocity starts to rise is the same. However, within about $10 \mu s$ of the velocity rise section, the velocity oscillation appears different processes due to the pressure reflection in the shell, which makes the final velocity of expansion different. Among the five metals, the final expansion speed and maximum pressure of copper shell are the largest, followed by steel shell, titanium alloy shell, and aluminum shell, showing a trend of decreasing with the decrease of density. The internal pressure of the shell decreases with the decrease of the density of the shell, and the amplitude and frequency of the reflection pulse decrease at the same time.

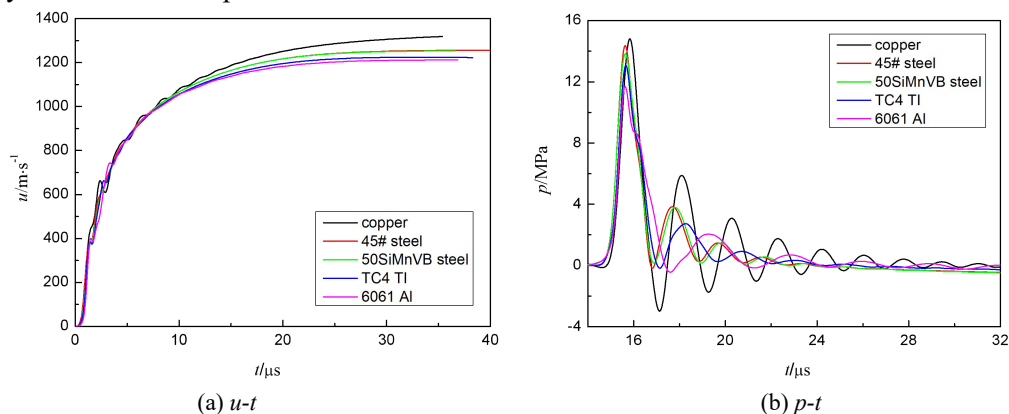


Figure 5. Expansion velocity and pressure curves of different metal shells with the same β value.

Table 2. Computational data for simulation of metal shells with $\beta=0.34$.

parameter	copper	45# steel	50SiMnVB steel	TC4 Ti	6061 Al
$u_{\max}/\text{m}\cdot\text{s}^{-1}$	1322.5	1256.4	1252.7	1224.8	1206.6
p_{\max}/GPa	14.572	14.366	13.831	13.075	11.701

The pressure nephogram inside the metal shell of five materials at the time of $t=20\mu\text{s}$ is shown in figure 6, indicative of the multiple reflection of the pressure wave inside the shell after the shock wave loading. The oxygen free copper shell has five clear periodic oscillation reflections. The two kinds of steel shells are basically the same, with three periodic oscillation reflections and incomplete subsequent reflections. The titanium alloy shell reflects in two periodic oscillations, and the subsequent reflection is not complete. The aluminum alloy shell has the lowest density and relatively thick thickness. After a complete periodic reflection, the second reflection cannot reach the outer surface of the shell, and does not form a complete reflection. It can be seen that the role of shock wave in the shell is related to the density and thickness of the metal shell. The higher the density of the metal shell is, the greater the amplitude of reflection is, the more the number of pulsations is, the less the dissipation energy of shock wave in the shell is, and the more the contribution of shock wave loading to fragment velocity is.

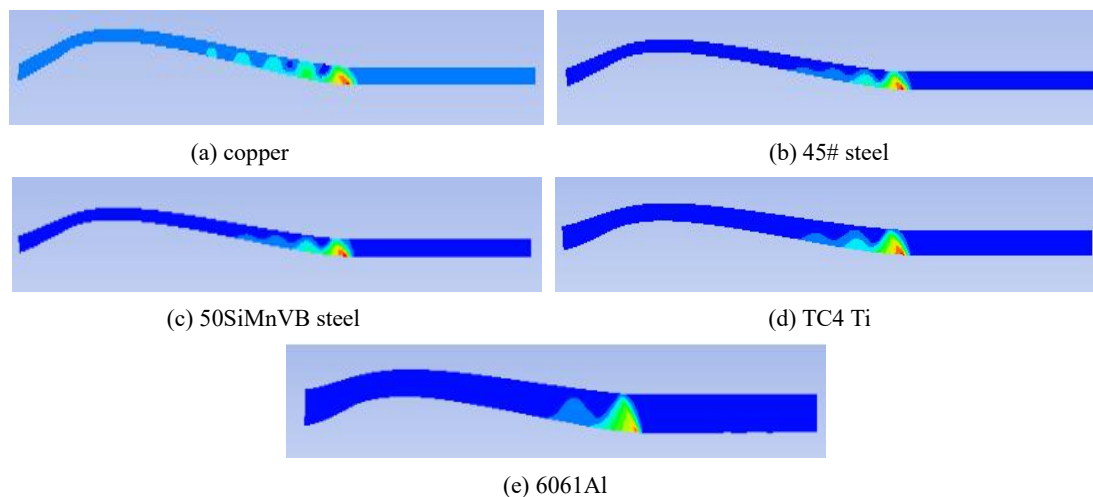


Figure 6. Pressure nephogram of different metal shells with the same β value at $t=20\mu\text{s}$.

According to the analysis of the simulation results, in the initial detonation stage, the surface velocity in the shell is greater than that in the outer surface. Because the shock wave propagates in the shell, the minimum value of the outer surface velocity just corresponds to the maximum value of the inner surface. With the expansion, the final velocity value of the inner and outer surface will tend to be the same. However, the inner surface is always in the compression state under the detonation loading, and the outer surface is in the compression and then tension state. Table 3 shows the maximum pressure values PN Max and PW Max reached by the inner and outer surface of five kinds of metal shells and the time when they appear. For the metal shells with the same β value, the maximum pressure difference between the inner and outer surface increases with the decrease of the density and the increase of the wall thickness of the metal materials, That is to say, the larger the energy dissipation of shock wave driving shell is, the smaller the acceleration obtained by the corresponding shock wave driving metal shell is, the smaller the speed obtained by the metal shell under the shock

wave loading is.

Table 3. Computational data of pressure on the inner and outer surfaces of metal shells with $\beta=0.34$.

parameter	copper	45# steel	50SiMnVB steel	TC4 Ti	6061 Al
p_{n-max} /GPa	17.474	17.111	16.814	16.793	16.631
t_{n-max} / μ s	15.33	15.266	15.281	15.157	15.097
p_{w-max} /GPa	4.0222	2.9434	2.7227	1.9905	1.4495
t_{w-max} / μ s	16.037	15.876	15.871	15.978	16.085
Δp /GPa	13.452	14.168	14.091	14.803	15.182

3.2. Effect Of Different β Values On Detonation Driven Metal Expansion

When the explosive load is the same explosive with the same charge structure, the larger the β value is, the larger the initial velocity of fragments is. However, by analyzing the detailed process of detonation driven metal shell expansion, the metal shell expands under the joint loading of shock wave and detonation products. When the thickness of the metal shell changes, the β value will change. On the one hand, the gurney velocity determined by this standard test will deviate when it is used in the structure of other β values; on the other hand, the thickness of the metal shell will change the shock wave and the loading of detonation products, and the calculation of fragment velocity will deviate greatly under the joint action of the two sides.

In order to discuss the influence of different β values, the numerical simulation of the oxygen-free copper shell and the 45# steel shell driven by TNT explosive detonation was carried out. The shell thickness increases from thin to thick, corresponding to β values of 1.0, 0.72, 0.50, 0.34, 0.22 and 0.15 respectively. The shell expansion speed curves of different β values are shown in figure7. It can be seen from figure7 that for different β values, the velocity shows obvious difference in the rising section. With the decrease of β value, the slope of the rising section of the curve is smaller, i.e. the acceleration of the rising section is smaller, indicating that the acceleration effect of shock wave loading on the metal shell is smaller with the increase of the thickness of the shell, and the velocity fluctuation of the velocity curve is more obvious. When $\beta = 1$, the thickness of the metal shell is the thinnest. At this time, the shock wave is reflected very fast in the shell, and the pulse process of the shock wave is completed rapidly. With the decrease of β value, the thickness of the shell increases, the pulse process lasts for a long time, the pulse period is relatively complete, and the velocity curve shows the wave phenomenon.

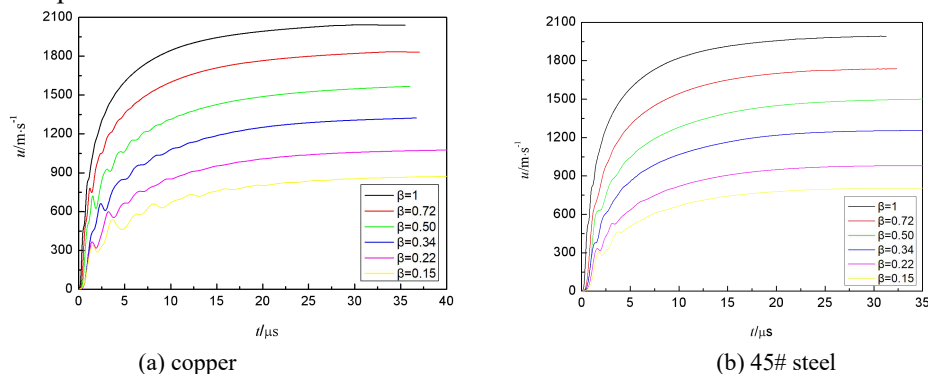


Figure 7. Velocity curves of metal shells with different β values.

The initial velocity of each model is calculated by Gurney formula, and the comparison results of the initial velocity of fragments and the maximum expansion velocity calculated by simulation model are shown in table 4. Based on the $\beta = 0.34$ copper shell corresponding to the standard cylinder test structure, the deviation between the initial velocity of fragments calculated by Gurney formula and the actual maximum expansion velocity is recorded as $\delta = (u_{\max} - v_0) / v_0$. It can be seen from table 4 that the calculation deviation of the thin-walled shell made of oxygen free copper material is positive, and the positive deviation increases with the increase of β value. However, the calculation deviation of the thick wall shell made of oxygen free copper is negative and increases with the decrease of β value. For the 45# steel shell, the initial velocity of fragments calculated by Gurney formula is higher than the actual expansion fragment velocity, and the velocity deviation of all models is negative deviation, and the negative deviation increases with the decrease of β value. This is because in the process of detonation driven expansion of steel shell, in addition to the influence of β value, there is also the influence of shell material. The common result of the two influences will cause a greater deviation in the initial velocity value of fragments calculated by Gurney formula.

Table 4. Comparison between the maximum velocity and the fragment velocity calculated by Gurney formula of copper shell and 45# steel shell with different β values.

parameter	$\beta=1$	$\beta=0.72$	$\beta=0.50$	$\beta=0.34$	$\beta=0.22$	$\beta=0.15$
Gurney initial velocity $v_0 / \text{m} \cdot \text{s}^{-1}$	2003.4	1785.3	1551.8	1322.5	1092.3	916.5
Copper $u_{\max} / \text{m} \cdot \text{s}^{-1}$	2065.5	1813.0	1564.7	1322.5	1081.4	880.2
δ_1	+3.10%	+1.55%	+0.83%	0	-0.99%	-3.66%
45# steel $u_{\max} / \text{m} \cdot \text{s}^{-1}$	1991.1	1737.7	1501.7	1256.4	980.9	804.4
δ_2	-0.61%	-2.67%	-3.23%	-5.0%	-10.20%	-12.23%

From the results of velocity analysis, it can be seen that the energy conversion of the expansion process of 45# steel shell is also different due to the influence of shell material and β value. For further analysis, the internal and external surface pressure curves of 45# steel shell with different β values calculated by simulation are shown in figure 8. As shown in figure 8, the solid line is the surface pressure curve inside the shell, and the dotted line is the surface pressure curve outside the shell. It can be seen from figure 8 that, due to the same charge structure, the time when the detonation wave propagates to the inner surface of the shell is the same, and the inner surface is in compression state, but with the increase of thickness, the pressure amplitude on the inner surface increases, the thicker the wall is, the slower the pressure amplitude increases, and the slower the attenuation is. The pressure curve of the outer surface of the shell varies greatly. The pressure curve of the outer surface of the shell with $\beta = 1$ has the largest amplitude and is basically in the state of compression. With the decrease of β value, the thickness of shell increases, and the amplitude of external surface pressure curve decreases gradually, and it turns to tensile state. Table 5 shows the maximum pressure amplitude and the time when the pressure curve on the internal and external surfaces of 45 steel shells with different β values reaches. It can be seen that with the decrease of β value, the pressure amplitude

difference between the internal and external surface becomes larger and larger, which also shows that the more energy the shock wave dissipates in the metal shell, the less energy is used to drive the shell to accelerate.

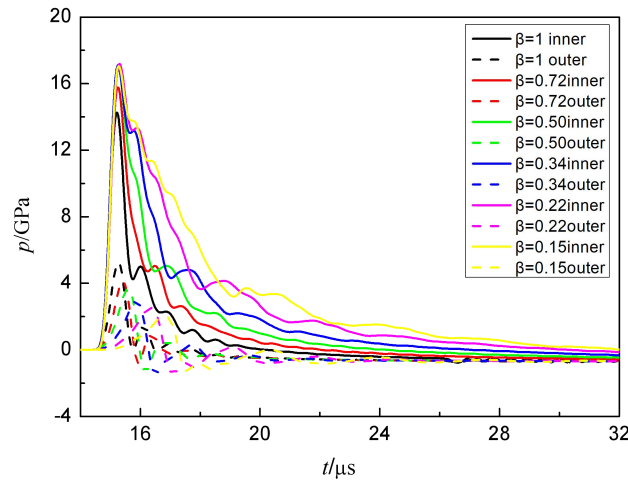
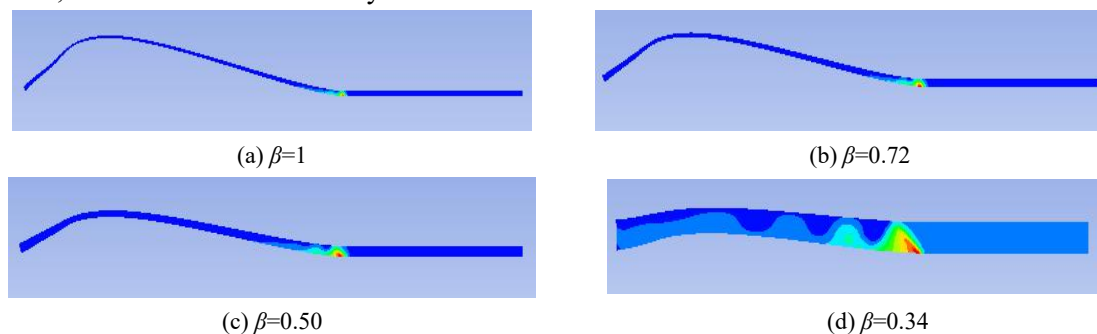


Figure 8. Pressure curves of inner and outer surfaces of 45# steel shells with different β values.

Table 5. Computational pressure data of inner and outer surface of 45# steel shells with different β values.

β	$\beta=1$	$\beta=0.72$	$\beta=0.50$	$\beta=0.34$	$\beta=0.22$	$\beta=0.15$
p_{n-max} /GPa	13.902	15.780	16.934	17.111	17.192	17.247
t_{n-max} / μ s	15.244	15.255	15.258	15.266	15.303	15.279
p_{w-max} /GPa	5.137	4.119	3.644	2.943	2.541	2.052
t_{w-max} / μ s	15.291	15.425	15.586	15.876	16.347	16.800
Δp /GPa	8.763	11.661	13.290	14.168	14.651	15.195

Figure 9 is the pressure nephogram of 45# steel shell with different β values at 20μ s. It can be seen from figure 9 that the shock wave loading process of thin-walled shell is extremely fast, the speed curve rises abruptly, and the acceleration is the largest. With the decrease of β value, the increase of shell thickness makes the reflection attenuation time and energy consumption of shock wave increase. In addition, the reflected pulse width of shock wave in the shell increases with the thickness of the shell, and also dissipates the energy of shock wave. These factors reduce the energy used to accelerate the shell, i.e. the acceleration ability of shock wave to the thick wall shell decreases.



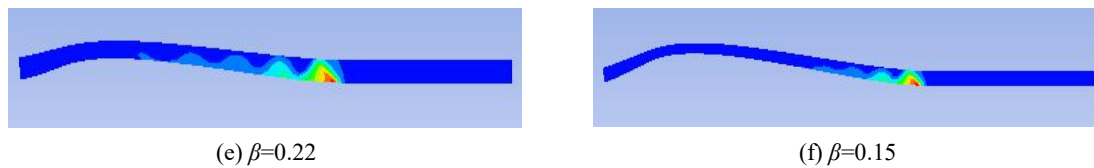


Figure 9. Pressure nephogram of 45# steel shells with the different β values at $t=20\mu\text{s}$.

4. Conclusion

In this paper, by using the numerical simulation method with AUTODYN software, through the detonation driving numerical simulation of different shell materials and different load coefficients, the curves of expansion speed and pressure change on the inner and outer surface of the shell, as well as the details of multiple reflection of stress wave in the shell, were obtained, and the influence law of metal shell materials and load coefficient β on fragment velocity was revealed. The main conclusions are as follows:

(1) The detonation with the same explosive load drives the metal shell with the same β value of different materials, and the maximum velocity of fragments is significantly different under the impact of shock wave loading effect. The higher the density of metal shell, the greater the reflection amplitude of shock wave in the shell, the more times of pulsation, the less the dissipation energy of shock wave in the shell, and the greater the contribution of shock wave loading to fragment velocity.

(2) With the increase of the thickness of the shell and the decrease of the corresponding load coefficient β , the larger the energy dissipated by the shock wave in the shell, the smaller the energy used to accelerate the shell expansion and the lower the contribution of the shock wave to the fragment velocity.

Reference

- [1] R W Gurney, 1943 *the Initial Velocities of Fragments from Bombs, Shells, and Grenades* Army Ballistic Research Laboratory, Report BRL 405, Aberdeen Proving Ground Maryland USA
- [2] Lee E L, Horning H C and Kury J W 1968 UCRL-50422 Livermore California
- [3] Kury J W, Hornig H C Lee E L, et al. 1965 Metal Acceleration by Chemical Explosives *4th Symp(Int) on Detonation White Oak MD*
- [4] Lindsay C M, Butler G C and Rumchik C G 2010 *Pro. Explosives Pyrotechnics* **35**(5) 433-9
- [5] John E. Reaugh and P Clark Souers 2004 *Propellants Explosives Pyrotechnics* **29**(2) 124-8
- [6] Predrag Elek and Slobodan Jaramaz 2013 *27th International symposium on ballistics Freiburg Germany April 22–26* 783-93
- [7] Matthew A Price¹, Vinh-Tan Nguyen¹ and Oubay Hassan 2016 *Int. J.For Numerical Methods in Engineering* **106** 904–26
- [8] Ren Guowei, Guo Zhaoliang and Zhang Shiwen et al. 2015 *Explosion and Shock Waves* **35**(6) 895-900
- [9] Yu Xinlu, Dong Xinlong and Fu Yingqian et al. 2014 *ACTA ARMAMENTARII*. **35**(2) 257-62
- [10] Liu Mingtao, Tang Tiegang and Hu Haibo et al. 2014 *Explosion and Shock Waves* **34**(4) 415-20
- [11] Wang Xinying, Wang Shushan and Ma Feng 2018 *International Journal of Impact Engineering* **114** 147–52